Journal of Power Sources 212 (2012) 226–232

Contents lists available at SciVerse ScienceDirect

Journal of Power Sources

journal homepage: www.elsevier.com/locate/jpowsour

Short communication

Sliding mode control of a linearized polymer electrolyte membrane fuel cell model

Gunhyung Park*, Zoran Gajic

Department of Electrical and Computer Engineering, Rutgers University, 94 Brett Road, Piscataway, NJ 08854-8058, USA

ARTICLE INFO

Article history:
Received 13 December 2011
Received in revised form
3 April 2012
Accepted 5 April 2012
Available online 13 April 2012

Keywords:
PEM fuel cell
Model linearization
Sliding mode control

ABSTRACT

The well-known nonlinear fifth-order model of a proton exchange membrane (PEM, also known as polymer electrolyte membrane) fuel cell (PEMFC) appears to be pretty complex. In this paper, we introduce the linearized model of the original nonlinear system and propose a sliding mode technique to keep the pressures of hydrogen and oxygen at the desired values despite of changes of the fuel cell current. Since the equilibrium point at steady state is unique, we perform Jacobian linearization of the original model at steady state and find the state space matrices of the linearized system using the MATLAB Symbolic Tool Box. The linearized system is asymptotically stable as well as controllable and observable. In this paper we show that a sliding mode control technique copes very well with the fuel cell external disturbance (changes of the fuel cell current) and produces excellent results for hydrogen and oxygen required pressures.

1. Introduction

Fuel cells are electrochemical energy devices that convert the chemical energy, during a hydrogen–oxygen reaction, into electricity, heat, and water. As a renewable energy source, fuel cells are one of the promising energy technologies with high efficiency and low environmental impact. Proton exchange membrane fuel cells are the most developed and popular type of fuel cells, using hydrogen as the fuel. PEMFC represents a nonlinear, multiple-input and multiple-output dynamic system [1].

Third-order models of PEMFC can be found in [2] (linear model) [3] (bilinear model), and [4] (nonlinear model). Na and Gou have derived a fifth-order nonlinear model [5] since Chiu et al. [4] indicated a need for using higher-order dimensional models of anode water (needed for membrane humidification) and cathode nitrogen, see Fig. 1. A nonlinear ninth-order model of PEMFC was derived in [6]. The model of [6] and its simplified fourth and sixth-order variants were considered in [7,8].

In the last few years, several control strategies for PEMFC are proposed. The sliding mode control technique that is robust against disturbances has been recently considered in several papers [7–15]. A second-order sliding mode controller is designed for the breathing subsystem of a PEMFC stack in [8], where the authors have focused on elimination of the chattering phenomenon. The model used in [8] is a nonlinear model of order six, which is derived based on the work of Pukrushpan et al. [6], Talj et al. [7], have first simplified and reduced the ninth-order model of [6] to a fourth-order highly nonlinear model and experimentally justified such a procedure. Then, they designed the corresponding sliding mode controller using as the sliding variable the difference between the actual and nominal angular air compressor speeds. The oxygen flow problem with real time implementation of a sliding mode controller has been considered for the first-order model that is obtained from the process input/output data in [12]. In [13], a hybrid controller composed of an internal mode control based PID controller and an adaptive sliding mode controller has been designed. The first controller is used to control the hydrogen reformer and the second controller is used to control the PEMFC model based on the work of [2]. A sliding mode control scheme is proposed for the DC/DC buck converter that guarantees a low and stable output voltage given transient variations in the output voltage of a PEMFC in [14]. A fuzzy sliding mode current controller of a hybrid fuel cell/energy-storage systems is considered in [10]. The method is presented for designing controllers for DC/DC and DC/AC converters. In [11], Hajizadeh and his coworkers used the fuel cell model of [11] coupled with a simple second-order model for the hydrogen reformer and a linear super capacitor model to design a sliding mode controller for active power under unbalanced voltage sag conditions. A sliding mode controller of DC/DC converters for a simplified dynamic model for fuel cells is used in [9]. Li et al. have presented a rapid-convergent sliding mode

* Corresponding author. Tel.: +1 732 609 2528; fax: +1 732 445 2820.
E-mail address: gunhyung.park@gmail.com (G. Park).

0378-7753/$ – see front matter
doi:10.1016/j.jpowsour.2012.04.014

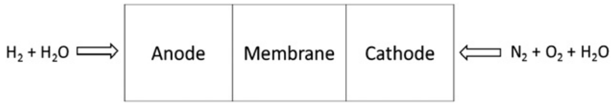

Fig. 1. Na and Gou 2008 model Schematic [5].

controller for the temperature control system of PEMFC stack [15]. That paper did not consider the fuel cell connection to an electric grid [9–11,14], but the model has included state variables that represent the fuel cell temperature [15].

In this paper we propose a sliding mode controller design for the fifth-order nonlinear model of PEMFC developed in [5], see also Ref. [16]. The state variables in this model represent respectively the pressures of hydrogen and water at the anode side and the pressures of oxygen, nitrogen, and water at the cathode side, that is

$$\begin{aligned} x(t) &= \left[P_{H_2}(t) \quad P_{H_2O_A}(t) \quad P_{O_2}(t) \quad P_{N_2}(t) \quad P_{H_2O_C}(t)\right]^T \\ &= [x_1(t) \quad x_2(t) \quad x_3(t) \quad x_4(t) \quad x_5(t)]^T \end{aligned} \tag{1}$$

The state space model is given by

$$\begin{aligned} \dot{x}_1 &= \frac{RT\lambda_{H_2}}{V_A}\left(Y_{H_2} - \frac{x_1}{x_1+x_2}\right) k_a u_a + \frac{RTC_1(1-\gamma)}{V_A}\left(\frac{x_1}{x_1+x_2} - 1\right) I \\ \dot{x}_2 &= \frac{RT\lambda_{H_2}}{V_A}\left(\frac{\varphi_a P_{vs}}{x_1+x_2-\varphi_a P_{vs}} - \frac{x_2}{x_1+x_2}\right) k_a u_a \\ &\quad + \frac{RTC_1}{V_A}\left(\frac{x_2}{x_1+x_2} - 1\right) I \\ \dot{x}_3 &= \frac{RT\lambda_{air}}{V_C}\left(Y_{O_2} - \frac{x_3}{x_3+x_4+x_5}\right) k_c u_c \\ &\quad + \frac{RTC_1}{2V_C}\left(\frac{x_3}{x_3+x_4+x_5} - 1\right) I \\ \dot{x}_4 &= \frac{RT\lambda_{air}}{V_C}\left(Y_{N_2} - \frac{x_4}{x_3+x_4+x_5}\right) k_c u_c \\ \dot{x}_5 &= \frac{RT\lambda_{air}}{V_C}\left(\frac{\varphi_c P_{vs}}{x_3+x_4+x_5-\varphi_a P_{vs}} - \frac{x_5}{x_3+x_4+x_5}\right) k_c u_c \\ &\quad + \frac{RTC(1-\gamma)}{V_C}\left(\frac{C_2}{C_1}\left(1 - \frac{x_5}{x_3+x_4+x_5}\right) - 1 - \frac{x_5}{x_3+x_4+x_5}\right) I \end{aligned} \tag{2}$$

where R is the universal gas constant, T is temperature, V_A, V_C and are anode and cathode volumes. C_1, C_2 are known constants [5,16], φ_a, φ_c are the relative humidity constants, P_{vs} is the saturation pressure, λ_{H_2}, λ_{air} and are stoichiometric constants, $Y_{H_2} = 0.99, Y_{O_2} = 0.21, Y_{N_2} = 0.79$, are reactant fractions. I is the cell current, and it is considered as a disturbance since it changes as V_{fc}/R_L, where V_{fc} is the produced fuel cell voltage and R_L is the load of active users, which changes randomly. γ is the coefficient measured experimentally in [17] for the back-diffusion of water from the cathode to the anode which is defined as $H_2O_{back} = \gamma H_2O_{mbr}$ where H_2O_{back} is the water back-diffusion flow rate and H_2O_{mbr} is the membrane water inlet flow rate [16]. In this model, it is assumed that the water in the system is perfectly controlled and the back-diffusion is not considered which means γ is zero.

The model output variables are defined by [5,16]

$$y(t) = \begin{bmatrix} P_{H_2}(t) \\ P_{O_2}(t) \end{bmatrix} = \begin{bmatrix} x_1(t) \\ x_3(t) \end{bmatrix} \tag{3}$$

The system control input is given by $u(t) = [u_a(t) \quad u_c(t)]^T$ where

$$u_a(t) = \frac{1}{k_a}(H_{2in}(t) + H_2O_{Ain}(t)) \tag{4}$$

$H_{2in}(t)$ and H_2O_{Ain} represent inlet flow rates of the anode side hydrogen and water vapor with k_a being a known constant, and

$$u_c(t) = \frac{1}{k_c}(O_{2in}(t) + N_{2in}(t) + H_2O_{Cin}(t)) \tag{5}$$

$O_{2in}(t)$, $N_{2in}(t)$ and $H_2O_{Cin}(t)$ represent respectively inlet flow rates of the cathode oxygen, nitrogen, and water with k_c being a known constant.

2. Linearization of PEM fuel cell dynamic model

Using MATLAB Symbolic Math Tool box, we obtain a unique equilibrium point for the given system (2) as

$$\begin{aligned} \bar{x}_1 &= \frac{\varphi_{11}}{\varphi_{12}}\varphi_a P_{vs}, \quad \bar{x}_2 = \frac{\varphi_{21}}{\varphi_{22}}\varphi_a P_{vs}, \quad \bar{x}_3 = \frac{\varphi_{31}}{\varphi_{32}}\varphi_c P_{vs}, \\ \bar{x}_4 &= \frac{\varphi_{41}}{\varphi_{42}}\varphi_c P_{vs}, \quad \bar{x}_5 = \frac{\varphi_{51}}{\varphi_{52}}\varphi_c P_{vs} \end{aligned} \tag{6}$$

Functions φ_{ij} are given in Appendix A.

Using the Jacobian linearization technique [18,19], the system (2) can be linearized at the equilibrium point. The Jacobian matrices at the equilibrium point defined by $\bar{x}$, $\bar{u}$, and $\bar{I}$, corresponding to system (2), and represented in general as $\dot{x} = f(x,u,I)$, are

$$\left.\frac{\partial f}{\partial s}\right|_{x=\bar{x},u=\bar{u},I=\bar{I}}, \quad \left.\frac{\partial f}{\partial u}\right|_{x=\bar{x},u=\bar{u},I=\bar{I}}, \quad \left.\frac{\partial f}{\partial I}\right|_{x=\bar{x},u=\bar{u},I=\bar{I}} \tag{7}$$

where

$$\begin{aligned} x(t) &= \bar{x} + \delta_x(t) \\ u(t) &= \bar{u} + \delta_u(t) \\ x(I) &= \bar{I} + \delta_I(t) \end{aligned} \tag{8}$$

The perturbations defined in (8) are assumed to be small [18,19]. The linearized system is defined by

$$\dot{\delta}_x(t) = A\delta_x(t) + B\delta_u(t) + G\delta_I(t) \tag{9}$$

with the constant matrices given by

$$\begin{aligned} A &= \left.\frac{\partial f}{\partial x}\right|_{x=\bar{x},u=\bar{u},I=\bar{I}} \in \mathbf{R}^{5\times 5}, \\ B &= \left.\frac{\partial f}{\partial u}\right|_{x=\bar{x},u=\bar{u},I=\bar{I}} \in \mathbf{R}^{5\times 2}, \\ G &= \left.\frac{\partial f}{\partial I}\right|_{x=\bar{x},u=\bar{u},I=\bar{I}} \in \mathbf{R}^{5\times 1} \end{aligned} \tag{10}$$

It has been found that the matrix A is given by

$$A = \left.\frac{\partial f}{\partial x}\right|_{x=\bar{x},u=\bar{u},I=\bar{I}} = \left.\begin{bmatrix} A_1 & 0_{2\times 3} \\ 0_{3\times 2} & A_2 \end{bmatrix}\right|_{x=\bar{x},u=\bar{u},I=\bar{I}} \tag{11}$$

where

$$A_1 = \begin{bmatrix} a_{11} & a_{12} \\ a_{21} & a_{22} \end{bmatrix}, \quad A_2 = \begin{bmatrix} a_{33} & a_{34} & a_{34} \\ a_{43} & a_{44} & a_{43} \\ a_{53} & a_{53} & a_{55} \end{bmatrix} \tag{12}$$

Elements a_{ij} are given in Appendix B.

The matrix B is similarly obtained as

$$B = \frac{\partial f}{\partial u}\bigg|_{x=\bar{x},u=\bar{u},I=\bar{I}} = \begin{bmatrix} b_{11} & 0 \\ b_{21} & 0 \\ 0 & b_{32} \\ 0 & b_{42} \\ 0 & b_{52} \end{bmatrix} \tag{13}$$

with elements b_{ij} given in Appendix C.

The matrix G is obtained as follows

$$G = \frac{\partial f}{\partial I}\bigg|_{x=\bar{x},u=\bar{u},I=\bar{I}} = \begin{bmatrix} g_1 \\ g_2 \\ g_3 \\ g_4 \\ g_5 \end{bmatrix} = \begin{bmatrix} \frac{RTC_1}{V_A}\left(\frac{\bar{x}_1}{\bar{x}_1+\bar{x}_2}-1\right) \\ \frac{RTC_1}{V_A}\left(\frac{\bar{x}_2}{\bar{x}_1+\bar{x}_2}-1\right) \\ \frac{RTC_1}{2V_C}\left(\frac{\bar{x}_3}{\bar{x}_3+\bar{x}_4+\bar{x}_5}-1\right) \\ 0 \\ \frac{RTC_1}{V_C}\left(\frac{C_2}{C_1}\left(1-\frac{\bar{x}_5}{\bar{x}_3+\bar{x}_4+\bar{x}_5}\right)-1-\frac{\bar{x}_5}{\bar{x}_3+\bar{x}_4+\bar{x}_5}\right) \end{bmatrix} \tag{14}$$

3. Sliding mode controller design of the linearized PEM fuel cell dynamic model

Sliding mode control is a form of variable structure control [20], where sliding surfaces are designed such that systems trajectories exhibit desirable properties. A system using sliding mode control has been considered as a robust system, which yields to reduced system sensitivity to uncertainties and exogenous disturbances.

Sliding mode control systems have been studied in different setups by many researchers [20]. The controller is designed in two steps – finding the sliding surface and reaching the sliding mode. After finding sliding surfaces using the method of [20] for linear systems or the Lyapunov method for nonlinear systems [21], the design of sliding mode control is achieved as follows. Firstly, a sliding surface is defined which ensures that the system remains on a hyperplane after reaching it from any initial condition in a finite time. Secondly, discontinuous control is designed to render a sliding mode. Approaches [20–23] can be used for continuous-time sliding mode control which has been recognized as a robust control approach, which yields to reject matched disturbances and system uncertainties. The matching condition [22], provided the control input makes the system asymptotically stable, assures robustness against parametric uncertainties and exogenous disturbances.

In the following, we present some basic concepts of the sliding mode control technique for linear systems such as the sliding surface design, sliding mode control design, and the disturbance rejection condition [23].

Consider a continuous-time linear system

$$\dot{x}(t) = Ax(t) + Bu(t) \tag{15}$$

where $x(t) \in \mathbf{R}^n$, $u(t) \in \mathbf{R}^m$, and A, B are constant matrices of appropriate dimensions, and B has full rank. There exists a similarity transformation defined by [20]

$$q(t) = Hx(t) \tag{16}$$

with

$$H = [N \quad B]^T \tag{17}$$

and columns of the $n \times (n-m)$ matrix N composed of basis vectors in the null space of B^T, which puts Equation (15) into the form

$$\dot{q}(t) = \bar{A}q(t) + \bar{B}u(t) \tag{18}$$

with $\bar{A} = HAH^{-1}$ and $\bar{B} = HB = \begin{bmatrix} 0 \\ \bar{B}_r \end{bmatrix}$. Equation (18) is decomposed as follows

$$\begin{bmatrix} \dot{q}_1(t) \\ \dot{q}_2(t) \end{bmatrix} = \begin{bmatrix} \bar{A}_{11} & \bar{A}_{12} \\ \bar{A}_{21} & \bar{A}_{22} \end{bmatrix}\begin{bmatrix} q_1(t) \\ q_2(t) \end{bmatrix} + \begin{bmatrix} 0 \\ \bar{B}_r \end{bmatrix}u(t) \tag{19}$$

where $q_1(t) \in \mathbf{R}^{n-m}$, $q_2(t) \in \mathbf{R}^m$, and $\bar{B}_r$ is an $m \times m$ nonsingular matrix.

Equation (19) yields

$$\dot{q}_1(t) = \bar{A}_{11}q_1(t) + \bar{A}_{12}q_2(t) \tag{20}$$

and

$$\dot{q}_2(t) = \bar{A}_{21}q_1(t) + \bar{A}_{22}q_2(t) + \bar{B}_r u(t) \tag{21}$$

$q_2(t)$ is treated as a control input to the system (20) and a state feedback gain K, which makes the system asymptotically stable, is defined by

$$q_2(t) = -Kq_1(t). \tag{22}$$

For the system (20), Utkin and Young have shown that $(\bar{A}_{11}, \bar{A}_{12})$ is controllable if and only if (A, B) is controllable [20], see also Ref. [24].

On the sliding surface, the system trajectory in the $(q_1(t), q_2(t))$ coordinates is expressed as

$$[K \quad I_m]\begin{bmatrix} q_1(t) \\ q_2(t) \end{bmatrix} = 0 \tag{23}$$

or

$$s(t) = [K \quad I_m]Hx(t) = Gx(t) = 0 \tag{24}$$

in the original coordinates. Consider the same system as in (15) with a disturbance $d(t)$

$$\dot{x}(t) = Ax(t) + Bu(t) + Ed(t) \tag{25}$$

The sliding variable dynamics is given by (the sliding surface is chosen as $s(t) = Gx(t)$)

$$\dot{s}(t) = G\dot{x}(t) = GAx(t) + GBu(t) + GEd(t) \tag{26}$$

The control law which satisfies the reaching condition directly can be chosen as

$$u(t) = -(GB)^{-1}GAx(t) - (GB)^{-1}(\gamma+\sigma)\left(\frac{s(t)}{\|s(t)\|}\right) \tag{27}$$

where

$$\gamma = \|GE\|d_{\max} \tag{28}$$

The disturbance matching condition [22], is given by

$$\mathrm{rank}([B \quad E]) = \mathrm{rank}([B]) \tag{29}$$

For the state space model (2), our objective is to keep y_{ref} in a certain range, which means to keep $e = y - y_{\text{ref}}$ around 0. We can define a sliding surface as follows

$$s = y - y_{\mathrm{ref}} \tag{30}$$

which yields

$$\dot{s} = \dot{y} - \dot{y}_{\mathrm{ref}} = \dot{y} = \begin{bmatrix} \dot{x}_1 \\ \dot{x}_3 \end{bmatrix} \tag{31}$$

The sliding mode control laws that satisfy $s\dot{s} < 0$ can be determined from Equations (32) and (33), will be presented in the next section.

Several other more complicated techniques for designing sliding surfaces and sliding mode controllers can be found in the engineering literature, see for example Refs. [25–27]. However, they are not needed for the purpose of this paper, since with the already introduced two standard and simple sliding mode techniques we get excellent results. As it will be shown in the simulation results, the chattering phenomenon (the main problem in using sliding mode control) will be fully suppressed and the abrupt changes of the fuel cell current (disturbance in a pretty broad range of 80 A–200 A) will have no impact on hydrogen and oxygen pressures.

4. Linearized PEM fuel cell dynamic model

4.1. Model linearization

The numerical data taken from [5], used in this paper, are presented in Table 1.

With the realistic numerical data in Table 1, we have found that the considered fuel cell system has a unique equilibrium point (steady state point) given by

$$\bar{x}(t) = [2.6509 \quad 0.0003 \quad 7.009 \quad 26.175 \quad 0.3390]^T \tag{32}$$

Table 1
Parameters of fuel cell.

Symbol	Parameter	Value [Unit]
R	Gas constant	8.314 [J mol^{-1} K^{-1}]
T	Operating cell temperature	353 [K]
N	Number of cells	35
V_A	Anode volume	0.005 [m^3]
V_C	Cathode volume	0.010 [m^3]
k_a	Anode conversion factor	7.034×10^{-4} [mol s^{-1}]
k_c	Cathode conversion factor	7.036×10^{-4} [mol s^{-1}]
A	Fuel cell active area	232×10^{-4} [m^2]
F	Faraday constant	96,485 [A s mol^{-1}]
P_{vs}	Saturation pressure	32 [kPa]
Y_{O_2}	O_2 reactant factor	0.2095
Y_{N_2}	N_2 reactant factor	0.7808
Y_{H_2}	H_2 reactant factor	0.9999
C_1	$N{\cdot}A/2F$	4.21×10^{-6} [m^2 mol A^{-1} s^{-1}]
C_2	$1.2684N{\cdot}A/F$	1.07×10^{-5} [m^2 mol A^{-1} s^{-1}]
λ_{H_2}	H_2 stoichiometric constant	2
λ_{air}	Air stoichiometric constant	2.5
φ_a	Anode humidity constant	0.8
φ_c	Cathode humidity constant	0.9
$H_{2\mathrm{in}}$	H_2 inlet flow rate	0.0611 [m^3 s^{-1}]
H_2O_{Ain}	H_2O inlet flow rate (Anode)	0.0019 [m^3 s^{-1}]
$O_{2\mathrm{in}}$	O_2 inlet flow rate	4.5403 [m^3 s^{-1}]
$N_{2\mathrm{in}}$	N_2 inlet flow rate	0.1503 [m^3 s^{-1}]
H_2O_{Cin}	H_2O inlet flow rate (Cathode)	0.0019 [m^3 s^{-1}]
I	Cell current density	100 [A m^{-2}]

The corresponding linearized system is

$$\dot{\delta}_x(t) = \begin{bmatrix} -8.741\times10^{-7} & 0.00782 & 0 & 0 & 0 \\ -0.00102 & -0.00884 & 0 & 0 & 0 \\ 0 & 0 & -0.02767 & 0.00732 & 0.00732 \\ 0 & 0 & 0.02733 & -0.00767 & 0.02733 \\ 0 & 0 & 0.00005 & 0.00005 & -0.03508 \end{bmatrix} \times \delta_x(t) + \begin{bmatrix} 9.5846\times10^{-8} & 0 \\ 8.5750\times10^{-4} & 0 \\ 0 & 2.0935\times10^{-6} \\ 0 & 2.9127\times10^{-3} \\ 0 & -6.3572\times10^{-6} \end{bmatrix} \delta_u(t) + \begin{bmatrix} 2.7255\times10^{-9} \\ -2.4384\times10^{-5} \\ -9.6493\times10^{-6} \\ 0 \\ 8.1233\times10^{-5} \end{bmatrix} \delta_I(t) = A\delta_x(t) + B\delta_u(t) + G\delta_I(t) \tag{33}$$

By examining the eigenvalues of the matrix A we found that all of them are in the left half complex plane, so that this system is open-loop asymptotically stable. The output equation according to Equation (3) has been already defined in the linear form in [5] and [16] as

$$y(t) = Cx(t) \tag{34}$$

with

$$C = \begin{bmatrix} 1 & 0 & 0 & 0 & 0 \\ 0 & 0 & 1 & 0 & 0 \end{bmatrix} \tag{35}$$

Having obtained matrices A, B, and C, we can examine the controllability and observability of the linearized system [28]. The controllability can be examined by studying the rank of the controllability matrix defined by [28]

$$C_o = \begin{bmatrix} B & AB & A^2B & A^3B & A^4B \end{bmatrix} \tag{36}$$

It was found that the rank of the controllability matrix is equal to 5, equal to the order of the system, $n = 5$, and hence this system is controllable. In other words, control inputs exist that can transfer the state of the system from any location in the state space to any desired location in the state space [28]. The system observability is tested by examining the rank of the observability matrix defined by [28]

$$O = \begin{bmatrix} C \\ CA \\ CA^2 \\ CA^3 \\ CA^4 \end{bmatrix} \tag{37}$$

It was found that the rank of the observability matrix is equal to 5 (equal to the order of the system), and this system is also observable [28].

4.2. Sliding mode controller design

The system in Equation (33) can be divided into two subsystems as follow

$$\begin{bmatrix} \dot{\delta}_{x_1}(t) \\ \dot{\delta}_{x_2}(t) \end{bmatrix} = \begin{bmatrix} -8.741 \times 10^{-7} & 0.00782 \\ -0.00102 & -0.00884 \end{bmatrix} \begin{bmatrix} \delta_{x_1}(t) \\ \delta_{x_2}(t) \end{bmatrix} + \begin{bmatrix} 9.5846 \times 10^{-8} \\ 8.5750 \times 10^{-4} \end{bmatrix} \delta_{u_a}(t) + \begin{bmatrix} 2.7255 \times 10^{-9} \\ -2.4384 \times 10^{-5} \end{bmatrix} \delta_I(t) = A_1 \delta_x(t) + B_1 \delta_u(t) + G_1 \delta_I(t) \tag{38}$$

$$\begin{bmatrix} \dot{\delta}_{x_1}(t) \\ \dot{\delta}_{x_2}(t) \\ \dot{\delta}_{x_3}(t) \end{bmatrix} = \begin{bmatrix} -0.02767 & 0.00732 & 0.00732 \\ 0.02733 & -0.00767 & 0.02733 \\ 0.00005 & 0.00005 & -0.03508 \end{bmatrix} \begin{bmatrix} \delta_{x_3}(t) \\ \delta_{x_4}(t) \\ \delta_{x_5}(t) \end{bmatrix} + \begin{bmatrix} 2.0935 \times 10^{-6} \\ 2.9127 \times 10^{-3} \\ -6.3572 \times 10^{-6} \end{bmatrix} \delta_{u_c}(t) + \begin{bmatrix} -9.6493 \times 10^{-6} \\ 0 \\ 8.1233 \times 10^{-5} \end{bmatrix} \delta_I(t) = A_2 \delta_x(t) + B_2 \delta_u(t) + G_2 \delta_I(t) \tag{39}$$

The objective is to keep the pressure differences of hydrogen and oxygen in a certain range to protect the membrane damage. We have designed the controller to keep both pressures around 3 atm.

For the first subsystem of Equation (38), there exists a nonsingular similarity transformation T_1 [20], which yields

$$\begin{bmatrix} \dot{q}_1(t) \\ \dot{q}_2(t) \end{bmatrix} = \begin{bmatrix} -1.6346 \times 10^{-6} & -9.1207 \\ 8.7110 \times 10^{-7} & -8.8370 \times 10^{-3} \end{bmatrix} \begin{bmatrix} q_1(t) \\ q_2(t) \end{bmatrix} + \begin{bmatrix} 0 \\ 7.3531 \times 10^{-7} \end{bmatrix} (u_a(t) + dI(t)) \tag{40}$$

with $d = -2.8436 \times 10^{-2}$. The disturbance can be nullified using Drazenovic's invariance condition since $\text{rank}([B_1\ G_1]) = \text{rank}([B_1])$ [22,29].

The pair $(\overline{A}_{1_{11}}, \overline{A}_{1_{12}})$ is controllable since the original system is controllable [20]. Hence, we can find a state feedback gain matrix K_1 such that $\overline{A}_{1_{11}} - K_1 \overline{A}_{1_{12}}$ is asymptotically stable.

On the sliding surface [20], the system trajectory in the ($q_1(t)$, $q_2(t)$) coordinates is expressed as

$$[K_1 \quad 1] \begin{bmatrix} q_1(t) \\ q_2(t) \end{bmatrix} = [-0.5482 \quad 1] \begin{bmatrix} q_1(t) \\ q_2(t) \end{bmatrix} = 0 \tag{41}$$

or

$$s_1(t) = [0.5482 \quad 1] T_1 \begin{bmatrix} x_1(t) \\ x_2(t) \end{bmatrix} = G_1 \begin{bmatrix} x_1(t) \\ x_2(t) \end{bmatrix} = 0.5482 x_1(t) + 7.9622 \times 10^{-4} x_2(t) = 0 \tag{42}$$

in the original coordinates.

Starting with $\dot{s}_1(t) = 0$, we design the sliding mode control law for the sliding surface (42)

$$\dot{s}_1(t) = 0 = G_1 \begin{bmatrix} \dot{x}_1 \\ \dot{x}_2 \end{bmatrix} = G_1 A_1 \begin{bmatrix} x_1(t) \\ x_2(t) \end{bmatrix} + G_1 B_1 (u_1(t) + dI(t)) \tag{43}$$

From Equation (43) and using the result of Equation (42), control $u_1(t)$ is obtained as

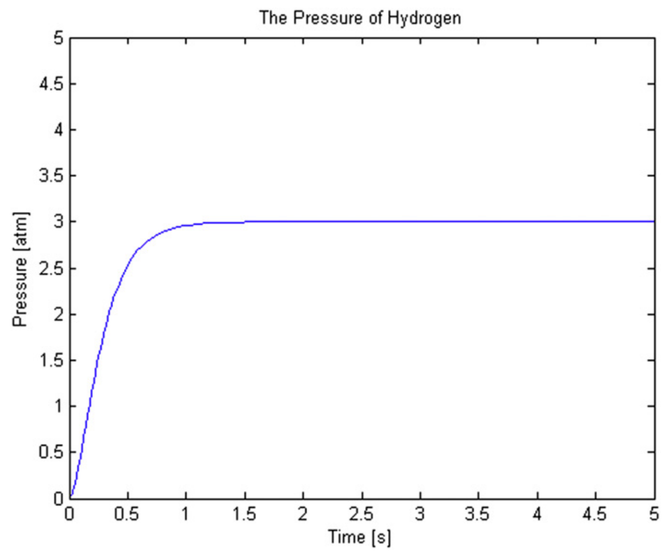

Fig. 2. Pressure of hydrogen of the linearized system.

$$u_1(t) = -(G_1 B_1)^{-1} G_1 A_1 \begin{bmatrix} x_1(t) \\ x_2(t) \end{bmatrix} - (G_1 B_1)^{-1} (\gamma_1 + \sigma_1) \frac{s_1(t)}{\|s_1(t)\|} \tag{44}$$

where

$$\gamma_1 = \|G_1 B_1\| dI_{\max} \tag{45}$$

is required to overcome the disturbance $I(t)$ and $\sigma_1 > 0$ provides that

$$s_1(t) \dot{s}_1(t) < 0 \tag{46}$$

is satisfied.

The second subsystem (39) does not satisfy Drazenovic's invariance condition. Instead of using Utkin and Young's method [20], we define the sliding surface for the second subsystem as

$$s_2(t) = y_2(t) - y_{2\text{ref}}(t) \tag{47}$$

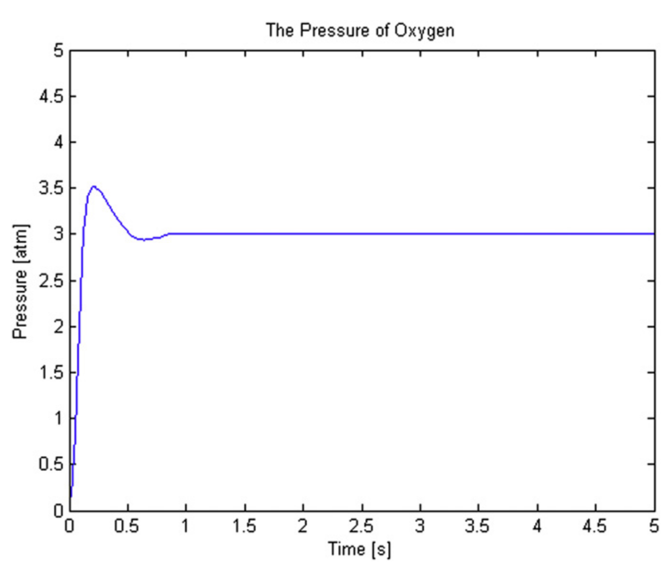

Fig. 3. Pressure of oxygen of the linearized system.

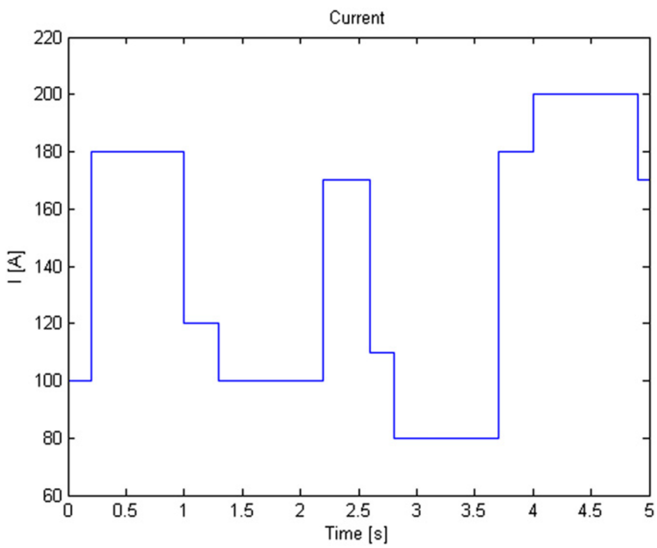

Fig. 4. Current changes.

similar with the method of Talj et al. [7]. Starting with $\dot{s}_2(t) = 0$, we design the sliding mode control law for the sliding surface defined in Equation (47)

$$\dot{s}_2(t) = 0 = \dot{y}_2(t) = \dot{x}_3(t)$$
$$= a_{33}x_3(t) + a_{34}x_4(t) + a_{34}x_5(t) + b_{32}u_c(t) + g_3 I(t) \quad (48)$$

From Equation (48), control $u_2(t)$ is obtained as

$$u_2(t) = -\frac{1}{b_{32}}(a_{33}x_3(t) + a_{34}x_4(t) + a_{34}x_5(t) + \sigma_2$$
$$+ |g_3| I_{\max} |s_2(t)| \quad (49)$$

where $\sigma_2 > 0$ is chosen to satisfy the condition

$$s_2\dot{s}_2 < 0 \quad (50)$$

Note that we can use the same procedure to find the sliding surface and the controller for the subsystem 1.

The simulation results are presented in Figs. 2 and 3. The disturbance current waveform is presented in Fig. 4.

In Fig. 2, the sliding mode control law is from Utkin and Young's method [20] and in Fig. 3, the control law is found by using $s = y_2 - y_{2\mathrm{ref}}$. It can be noticed from Figs. 2 and 3 that the pressures are kept around 3 atm after about 1 s despite the current density changes during entire time internal of interest, from 0 to 5 s.

5. Conclusion

We have applied the sliding mode strategy for the linearized model of the well-known nonlinear model of the proton exchange membrane fuel cell obtained using the MATLAB Symbolic Tool Box. For this well defined model, which has uniqueness of steady state variables, asymptotic stability, controllability, and observability, the sliding mode technique copes very well with the cell current changes $I(t)$, and keeps very precisely the pressures of hydrogen and oxygen at the desired (required) values.

Appendix A

$$\varphi_{11} = C_1^2 I^2 - 2\lambda_{H_2} C_1 I (Y_{H_2} - 1) k_a u_a + \lambda_{H_2}^2 Y_{H_2}(Y_{H_2} - 2) k_a^2 u_a^2$$

$$\varphi_{12} = C_1^2 I^2 - \lambda_{H_2} C_1 I Y_{H_2} k_a u_a + \lambda_{H_2}^2 (Y_{H_2} - 1) k_a^2 u_a^2$$

$$\varphi_{21} = \lambda_{H_2} C_1 I (Y_{H_2} - 1) k_a u_a - \lambda_{H_2}^2 \left(Y_{H_2}^2 - 3Y_{H_2} + 2\right) k_a^2 u_a^2$$

$$\varphi_{22} = C_1^2 I^2 - \lambda_{H_2} C_1 I Y_{H_2} k_a u_a + \lambda_{H_2}^2 (Y_{H_2} - 1) k_a^2 u_a^2$$

$$\begin{aligned}\varphi_{31} = {} & I^2 C_1^2 (-C_1 + C_2 + (C_1 + C_2) Y_{N_2}) + \lambda_{\mathrm{air}} I^2 C_1 (3C_1 \\ & - (C_1 + 2C_2) Y_{N_2})(-4C_2 Y_{O_2} - 2(C_1 + C_2) Y_{N_2} Y_{O_2}) k_c u_c \\ & + 2\lambda_{\mathrm{air}}^2 I \Big(2C_1 - C_1 Y_{N_2} - 4C_1 Y_{O_2} + 2(C_1 + C_2) Y_{O_2}^2 \\ & + (C_1 + 2C_2) Y_{N_2} Y_{O_2}\Big) k_c^2 u_c^2 + 4\lambda_{\mathrm{air}}^3 (Y_{N_2} + Y_{O_2} \\ & - 2) Y_{O_2} k_c^2 u_c^2 Y_{O_2}\end{aligned}$$

$$\begin{aligned}\varphi_{32} = {} & I^3 C_1^2 (-C_1 + C_2 + (C_1 + C_2) Y_{N_2}) + \lambda_{\mathrm{air}} I^2 C_1 (\\ & - 2(3C_1 - C_2) + (3C_1 + 4C_2) Y_{N_2} + 2(C_1 + C_2) Y_{O_2}) k_c u_c \\ & + 2\lambda_{\mathrm{air}}^2 I (2C_2 Y_{N_2} + (C_1 + 2C_2) Y_{O_2} - 3C_1) k_c^2 u_c^2 + 4\lambda_{\mathrm{air}}^3 (Y_{N_2} \\ & + Y_{O_2} - 1) k_c^3 u_c^3\end{aligned}$$

$$\begin{aligned}\varphi_{41} = {} & I^2 C_1 Y_{N_2} ((C_1 - C_2) - (C_1 + C_2) Y_{N_2}) \\ & + \lambda_{\mathrm{air}} I Y_{N_2} (-3C_1 + (C_1 + 2C_2) Y_{N_2})(2(C_1 + C_2) Y_{O_2}) k_c u_c \\ & + 2\lambda_{\mathrm{air}}^2 (-2 + Y_{N_2} + Y_{O_2}) Y_{N_2} k_c^2 u_c^2\end{aligned}$$

$$\begin{aligned}\varphi_{42} = {} & I^2 C_1 ((C_1 - C_2) - (C_1 + C_2) Y_{N_2}) + \lambda_{\mathrm{air}} I Y_{N_2} (-4C_1 \\ & + (C_1 + 2C_2) Y_{N_2})(2(C_1 + C_2) Y_{O_2}) k_c u_c \\ & + 2\lambda_{\mathrm{air}}^2 (-1 + Y_{N_2} + Y_{O_2}) k_c^2 u_c^2\end{aligned}$$

$$\begin{aligned}\varphi_{51} = {} & I^3 C_1^2 Y_{N_2} (C_1 - C_2 - (C_1 + C_2) Y_{N_2}) + \lambda_{\mathrm{air}} I^2 C_1 (B_1 + B_2 + B_3 \\ & + B_4) k_c u_c - 2\lambda_{\mathrm{air}}^2 I (B_5 + B_6 + B_7) k_c^2 u_c^2 - 4\lambda_{\mathrm{air}}^3 (2 + Y_{N_2} \\ & + Y_{O_2})(1 + Y_{N_2} + Y_{O_2}) k_c^3 u_c^3\end{aligned}$$

$$B_1 = 2(C_1 - C_2) - 7C_1 Y_{N_2}; \quad B_2 = -2(C_1 - C_2) Y_{O_2}$$

$$B_3 = 4(C_1 + C_2) Y_{N_2} Y_{O_2}; \quad B_4 = (3C_1 + 4C_2) Y_{N_2}^2$$

$$B_5 = 3C_1 + 2(C_1 - C_2) Y_{N_2}; \quad B_6 = -(5C_1 + 2C_2) Y_{O_2} + 2C_2 Y_{N_2}^2$$

$$B_7 = 2(C_1 + C_2) Y_{O_2}^2 + 2(C_1 + 2C_2) Y_{N_2} Y_{O_2}$$

$$\begin{aligned}\varphi_{52} = {} & I^3 C_1^2 (-C_1 + C_2 + (C_1 + C_2) Y_{N_2}) + \lambda_{\mathrm{air}} I^2 C_1 (\\ & - 2(3C_1 - C_2) + (3C_1 + 4C_2) Y_{N_2} + 2(C_1 + C_2) Y_{O_2}) k_c u_c \\ & + 2\lambda_{\mathrm{air}}^2 I (2C_2 Y_{N_2} + (C_1 + 2C_2) Y_{O_2} - 3C_1) k_c^2 u_c^2 + 4\lambda_{\mathrm{air}}^3 (Y_{N_2} \\ & + Y_{O_2} - 1) k_c^3 u_c^3\end{aligned}$$

Appendix B

$$a_{11} = \frac{RT}{V_A}\left(-\lambda_{H_2}k_a\bar{u}_a + C_1\bar{I}\right)\frac{\bar{x}_2}{(\bar{x}_1+\bar{x}_2)^2}$$

$$a_{12} = \frac{RT}{V_A}\left(\lambda_{H_2}k_a\bar{u}_a - C_1\bar{I}\right)\frac{\bar{x}_1}{(\bar{x}_1+\bar{x}_2)^2}$$

$$a_{21} = \frac{RT}{V_A}\lambda_{H_2}\left(\frac{-\varphi_a P_{vs}}{(\bar{x}_1+\bar{x}_2-\varphi_a P_{vs})^2} + \frac{\bar{x}_2}{(\bar{x}_1+\bar{x}_2)^2}\right)k_a\bar{u}_a - \frac{RT}{V_A}\left(C_1\bar{I}\frac{\bar{x}_2}{(\bar{x}_1+\bar{x}_2)^2}\right)$$

$$a_{22} = \frac{RT}{V_A}\lambda_{H_2}\left(\frac{-\varphi_a P_{vs}}{(\bar{x}_1+\bar{x}_2-\varphi_a P_{vs})^2} - \frac{\bar{x}_1}{(\bar{x}_1+\bar{x}_2)^2}\right)k_a\bar{u}_a + \frac{RT}{V_A}\left(C_1\bar{I}\frac{\bar{x}_1}{(\bar{x}_1+\bar{x}_2)^2}\right)$$

$$a_{33} = \frac{RT}{V_C}\left(-\lambda_{air}k_c\bar{u}_c - \frac{C_1}{2}\bar{I}\right)\frac{\bar{x}_4+\bar{x}_5}{(\bar{x}_3+\bar{x}_4+\bar{x}_5)^2}$$

$$a_{34} = \frac{RT}{V_C}\left(\lambda_{air}k_c\bar{u}_c - \frac{C_1}{2}\bar{I}\right)\frac{\bar{x}_3}{(\bar{x}_3+\bar{x}_4+\bar{x}_5)^2}$$

$$a_{43} = \frac{RT}{V_C}\lambda_{air}k_c\bar{u}_c\frac{\bar{x}_4}{(\bar{x}_3+\bar{x}_4+\bar{x}_5)^2}$$

$$a_{44} = \frac{RT}{V_C}\lambda_{air}k_c\bar{u}_c\frac{\bar{x}_3+\bar{x}_5}{(\bar{x}_3+\bar{x}_4+\bar{x}_5)^2}$$

$$a_{53} = \frac{RT}{V_C}\lambda_{air}\left(\frac{-\varphi_c P_{vs}}{(\bar{x}_3+\bar{x}_4+\bar{x}_5-\varphi_c P_{vs})^2} + \frac{\bar{x}_5}{(\bar{x}_3+\bar{x}_4+\bar{x}_5)^2}\right)k_c\bar{u}_c + \frac{RT}{V_C}(C_1+C_2)\,\bar{I}\frac{\bar{x}_5}{(\bar{x}_3+\bar{x}_4+\bar{x}_5)^2}$$

$$a_{55} = \frac{RT}{V_C}\lambda_{air}\left(\frac{-\varphi_c P_{vs}}{(\bar{x}_3+\bar{x}_4+\bar{x}_5-\varphi_c P_{vs})^2} - \frac{\bar{x}_3+\bar{x}_4}{(\bar{x}_3+\bar{x}_4+\bar{x}_5)^2}\right)k_c\bar{u}_c - \frac{RT}{V_C}(C_1+C_2)\,\bar{I}\frac{\bar{x}_3+\bar{x}_4}{(\bar{x}_3+\bar{x}_4+\bar{x}_5)^2}$$

Appendix C

$$b_{11} = \frac{RT}{V_A}\lambda_{H_2}\left(Y_{H_2} - \frac{\bar{x}_1}{\bar{x}_1+\bar{x}_2}\right)k_a$$

$$b_{21} = \frac{RT}{V_A}\lambda_{H_2}\left(\frac{\varphi_a P_{vs}}{\bar{x}_1+\bar{x}_2-\varphi_a P_{vs}} - \frac{\bar{x}_2}{\bar{x}_1+\bar{x}_2}\right)k_a$$

$$b_{32} = \frac{RT}{V_C}\lambda_{air}\left(Y_{O_2} - \frac{\bar{x}_3}{\bar{x}_3+\bar{x}_4+\bar{x}_5}\right)k_c$$

$$b_{42} = \frac{RT}{V_C}\lambda_{air}\left(Y_{N_2} - \frac{\bar{x}_4}{\bar{x}_3+\bar{x}_4+\bar{x}_5}\right)k_c$$

$$b_{52} = \frac{RT}{V_C}\lambda_{air}\left(\frac{\varphi_c P_{vs}}{\bar{x}_3+\bar{x}_4+\bar{x}_5-\varphi_a P_{vs}} - \frac{\bar{x}_5}{\bar{x}_3+\bar{x}_4+\bar{x}_5}\right)k_c$$

References

[1] J. Larminie, A. Dicks, Fuel Cell Systems Explained, John Wiley & Sons, Chichester, 2000.
[2] M.Y. El-Sharkh, A. Rahman, M.S. Alam, P.C. Byrne, A.A. Sakla, T. Thomas, Journal of Power Sources 138 (2004) 199–204.
[3] R.S. Gemmen, Journal of Fluids Engineering 125 (3) (2003) 576–585.
[4] L.-Y. Chiu, B. Diong, R. Gemmen, IEEE Transactions on Industry Applications 40 (4) (2004) 970–977.
[5] W. Na, B. Gou, IEEE Transactions on Energy Conversion 23 (2008) 179–190.
[6] J.T. Pukrushpan, A.G. Stefanopoulou, H. Peng, Control of Fuel Cell Power Systems, Springer, USA, 2004.
[7] R. Talj, D. Hissel, R. Ortega, M. Becherif, IEEE Transactions on Industrial Electronics 57 (2010) 1906–1913.
[8] C. Kunusch, P. Puleston, M. Mayosky, J. Riera, IEEE Transactions on Control Systems Technology 17 (1) (2009) 167–174.
[9] F. Zenith, S. Skogestad, Journal of Process Control 17 (4) (2007) 333–347.
[10] A. Hajizadeh, M. Golkar, Expert Systems with Applications 37 (2010) 7627–7638.
[11] A. Hajizadeh, M. Golkar, A. Feliachi, IEEE Transaction on Energy Conversion 25 (2010) 1195–1208.
[12] W. Garcia-Gaban, F. Dorado, C. Bordons, Journal of Process Control 20 (2010) 325–336.
[13] G. Wang, Y. Wang, J. Shi, H. Shao, ISA Transactions 49 (2010) 87–94.
[14] J.-K. Kuo, C.-F. Wang, International Journal of Hydrogen Energy 36 (18) (2011) 11846–11855.
[15] X. Li, Z.-H. Deng, D. Wei, C.-S. Xu, G.-Y. Cao, Energy Conversion and Management 52 (11) (2011) 3265–3274.
[16] B. Gou, W. Na, B. Diong, Fuel Cells: Modeling, Control, and Applications, CRC Press/Taylor and Francis Group, Boca Raton, Florida, USA, 2010.
[17] F. Barbir, PEM Fuel Cells: Theory and Practice, Elsevier Academic Press, New York, 2005.
[18] Z. Gajic, Linear Dynamic Systems and Signals, Prentice Hall, 2003.
[19] H. Khalil, Nonlinear Systems, Prentice Hall, 2002.
[20] V.I. Utkin, K.D. Young, Remote Control 39 (10) (1978) 1466–1470.
[21] W.-C. Su, S.V. Drakunov, Ü Özgüner, Automatica 32 (6) (1996) 925–928.
[22] B. Drazenovic, Automatica 5 (3) (1969) 287–295.
[23] A. Sinha, Linear Systems, CRC Press, Inc., Boca Raton, FL, USA, 2007.
[24] C.-T. Chen, Linear System Theory and Design, Oxford University Press, Inc., New York, NY, USA, 1999.
[25] S. Laghrouche, F. Plestan, A. Glumineau, Automatica 43 (3) (2007) 531–537.
[26] J.E. Slotine, W. Li, Applied Nonlinear Control, Prentice Hall, Englewood Cliffs, New Jersey, 1991.
[27] V.I. Utkin, J. Guldner, J. Shi, Sliding Mode Control in Electromechanical Systems, Taylor & Francis, London, 1999.
[28] Z. Gajic, M. Lelic, Modern Control Systems Engineering, Prentice Hall, 1996.
[29] W.-C. Su, International Journal of Control 72 (11) (1999) 990–995.